Isotopic signature of plutonium accumulated in glaciers worldwide

Edyta Łokas[1], Giovanni Baccolo[2], Anna Cwanek[1], Jakub Buda[3], Katarzyna Kołtonik[1], Nozomu Takeuchi[4], Przemysław Wachniew[5], Caroline Clason[6], Krzysztof Zawierucha[3], Dylan Bodhi Beard[7], Roberto Ambrosini[8], Francesca Pittino[9], Andrea Franzetti[9], Philip N. Owens[10], Massimiliano Nastasi[11,12], Monica Sisti[13], Biagio Di Mauro[14]

[1]*Institute of Nuclear Physics PAS, Department of Mass Spectrometry, Krakow, Poland*
[2]*Department of Science, Università degli Studi Roma Tre, 00146 Rome, Italy*
[3]*Department of Animal Taxonomy and Ecology, Faculty of Biology, Adam Mickiewicz University, Poznań, Poland*
[4]*Department of Earth Sciences, Chiba University, Chiba, Japan*
[5]*Faculty of Physics and Applied Computer Science, AGH University of Science and Technology, Krakow, Poland*
[6]*Department of Geography, Durham University, Durham, UK*
[7]*School of Geography, Earth and Environmental Sciences, University of Plymouth, Plymouth, UK*
[8]*Department of Environmental Science and Policy, University of Milano, Milan, Italy*
[9]*Università degli Studi di Milano-Bicocca, Milan, Italy*
[10]*Department of Geography, Earth and Environmental Sciences, University of Northern British Columbia, Prince George, Canada*
[11]*Physics Department, University of Milano-Bicocca, Piazza della Scienza 3, Milano 20126, Italy*
[12]*INFN section of Milano Bicocca, Piazza della Scienza 3, Milano 20126, Italy*
[13] *Institute of Polar Sciences, National Research Council, Milan, Italy*

Abstract

Glaciers are recognised as repositories for atmospheric pollutants, however, due to climate change and enhanced melting rates, they are rapidly transitioning from being repositories to secondary sources. Artificial radionuclides are one of the pollutants found on glaciers that efficiently accumulated onto glacier surfaces within cryoconite deposits (a dark, often biogenic sediment). The high concentrations of radionuclides in cryoconite allow the accurate investigation of low-activity artificial isotopes, including plutonium. This work provides information about the accumulation, distribution and sources of plutonium isotopes in cryoconite from glaciers worldwide. Samples collected from 50 glaciers across nine regions of Earth are considered. Activity concentrations of plutonium in cryoconite are orders of magnitude higher than in other environmental matrices, in particular in the Northern Hemisphere. Isotopic ratios indicate that plutonium contamination of cryoconite is mostly consistent with the global signal of stratospheric fallout related to atmospheric nuclear tests. However, specific glaciers in Svalbard reveal a signature compatible with a contribution from

the re-entry of the SNAP-9A satellite in 1964, which was equipped with a ^{238}Pu radioisotope thermoelectric generator. Similarly, an excess of ^{238}Pu was observed in cryoconite from the Exploradores Glacier (Chile). This could be associated with the November 1996 crash of the automatic Interplanetary Station "Mars'96" which was carrying a ^{238}Pu generator. This is the first time that isotopic evidence for this event has been reported. These findings highlight the role that cryoconite can play in reconstructing the radioactive contamination history of different glaciated regions of the Earth.

Keywords: glaciers, cryoconite, plutonium, activity ratio, mas ratio

Graphical abstract

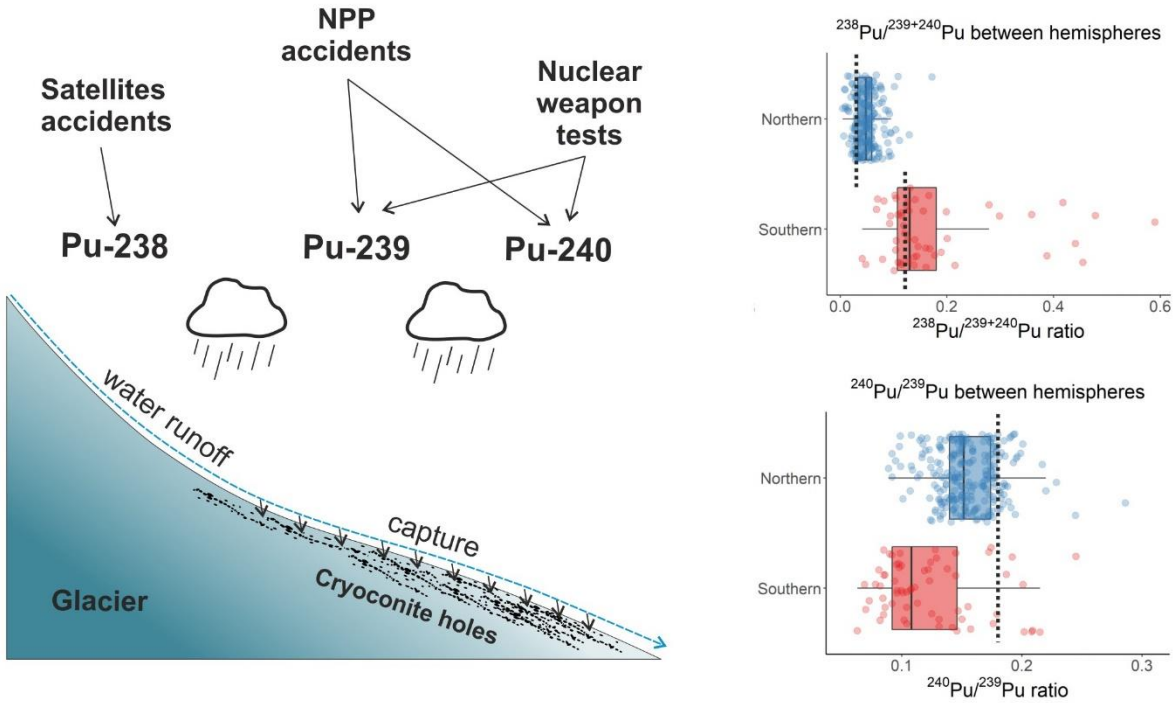

1. Introduction

Atmospherically-derived radioactivity is the component of environmental radioactivity that is deposited on the Earth's surface through wet and dry deposition from the atmosphere. The deposited radionuclides are also described as fallout radionuclides (FRNs). Some FRNs have a natural origin, such as cosmogenic ^{7}Be and ^{14}C, or are decay products of primordial isotopes like ^{210}Pb, which derives from ^{238}U. However, most FRNs are artificial and occur globally as a result of atmospheric nuclear tests and unintentional nuclear accidents (UNSCEAR, 1982,

2000). A key requirement when dealing with environmental radioactivity is the assessment of contamination levels, including the reconstruction of contamination histories and the identification of pathways and the fate of the released radioactivity (Engelbrecht and Schwaiger, 2008).

Glaciers are especially important for studying atmospheric fallout history (Jaworowski et al., 1978). First of all, glaciers consist of deposits of atmospheric precipitation and intrinsically accumulate fallout species, including FRNs. Under specific conditions (i.e. no melting, low horizontal ice flow), by studying the stratigraphy of ice and snow layers, it becomes possible to reconstruct the depositional history of FRNs (Gabrieli et al., 2011; Olivier et al., 2004). In addition to glacier ice, attention has recently turned to another environmental matrix typical of glaciated landscapes which accumulates radioactivity: cryoconite. Cryoconite is a sediment found on the surface of glaciers worldwide (Cook et al., 2016). It is composed of a dominant mineral fraction, and of auto- and allochthonous organic matter accounting for ca. 1.5-40% of cryoconite mass, which includes a range of living organisms and can form biogenic granules (Rozwalak et al., 2022; Wejnerowski et al., 2023). This supraglacial sediment is characterized by a remarkably low albedo compared to the surrounding ice (Di Mauro et al., 2017), and it has been recognized for its ability to efficiently accumulate environmental radioactivity (Łokas et al., 2017; Łokas et al., 2016), rapidly becoming a promising matrix for monitoring radioisotope pollution in high latitude and altitude sites (Clason et al., 2023; Clason et al., 2021). Many FRNs found in cryoconite samples have the highest activity concentrations ever reported in environmental materials from sites outside areas of nuclear tests and accidents (Baccolo et al., 2020; Buda et al., 2023; Clason et al., 2023; Łokas et al., 2022; Łokas et al., 2019; Łokas et al., 2018; Owens et al., 2019). The high concentrations of FRNs in cryoconite is likely related to the presence of metal-binding extracellular polymeric substances in its organic fraction (Nagar et al., 2021). However, the interaction of FRNs with ferromanganese oxides and mineral binding sites also plays a role in FRN accumulation (Buda et al., 2023).

Plutonium is a toxic, radioactive and predominately anthropogenic element produced through neutron irradiation of uranium in nuclear reactors and during nuclear weapon detonations (Zhong et al., 2019). The most significant releases of plutonium in the Northern Hemisphere were associated with global fallout resulting from atmospheric nuclear weapon tests carried out between 1945 and 1980, with a peak in the 1960s (UNSCEAR, 1982, 2000). Other important sources are related to catastrophic events such as the 1978 crash of the Cosmos-954 satellite, which had a nuclear reactor on board (Krey et al., 1979; Tracy et al., 1984), as well as the Chernobyl nuclear power plant disaster in 1986 (UNSCEAR, 2010) and the

Fukushima Daiichi accident in 2011 (Povinec et al., 2013a; Povinec et al., 2013b). Moreover, from 1964 to 1980, China conducted atmospheric nuclear testing at the Lop Nor test site in north-western China. The Northern Hemisphere has received two-thirds of global plutonium deposition (Clark et al., 2019). Signatures of individual tests and events vary regionally due to their different horizontal distribution and relative yields. Figure 1 illustrates the most significant atmospheric nuclear testing and accident sites in the Northern and Southern Hemispheres, including those near the Equator. The tests conducted in the Northern Hemispere have received significant interest but much less is known regarding the deposition that took place in the Southern Hemisphere. The United Kingdom (UK) was at the forefront of the atmospheric nuclear testing program in the Southern Hemisphere between 1952 and 1957 in Australian territory, while France conducted extensive open-air nuclear testing in French Polynesia in the South Pacific Ocean from 1966 to 1974. The UK tests resulted in a substantial amount of regional fallout (i.e., tropospheric fallout), compared to the higher-yield French tests, which contributed to the stratospheric fallout.

In 1964, the Transit 5BN3 satellite carrying a SNAP 9A radio-thermal generator, launched by the United States of America (USA), failed to achieve orbit. The satellite burned up when descending into the upper atmosphere over Madagascar. The ^{238}Pu load (corresponding to 1 kg) was dispersed worldwide and was detected globally in the environment, even in remote areas. Most of the fallout of ^{238}Pu from this satellite occurred in the Southern Hemisphere (Hardy et al., 1972, 1973). Another important event, although not well-documented, was reported by the International Atomic Energy Agency (Radiation and Safety, 2001) in their inventory of accidents and losses at sea involving radioactive material. According to the report, it involved the atmospheric re-entry of the automatic Interplanetary Station “Mars ’96”, which was launched on 16 November 1996. The station fell off the coast of Chile near the border with Bolivia and has not been located to date.

Plutonium isotope deposition after weapons testing can be local, regional and global, depending on detonation height, yield and meteorological conditions (Wendel et al., 2013). However, the source of plutonium isotopes is defined by specific signatures of different ratios, as presented in Table 1. This study, for the first time, presents a comprehensive global analysis of the variation in activity concentrations of ^{238}Pu and $^{239+240}$Pu, along with activity (^{238}Pu/$^{239+240}$Pu) and atomic (^{240}Pu/^{239}Pu) ratios, observed in cryoconite on glaciers from both hemispheres. To understand whether the accumulation of plutonium isotopes is influenced by factors other than local sources, we relate the activity concentrations of ^{238}Pu and $^{239+240}$Pu with geographical and compositional variables of cryoconite, such as its organic matter content,

elevation of the sampling sites, and glacier-type (e.g. outlet or valley). Moreover, because the overall peak in stratospheric deposition of anthropogenic radionuclides was between January 1962 and December 1964, we also consider total precipitation for this period. Using such an approach, it was possible to describe the variability of plutonium isotopes in cryoconite depending on the geographic and climatic context. Furthermore, for the first time, an excess of ^{238}Pu was identified in southern Chile, possibly related to the crash of the Automatic Interplanetary Station "Mars '96" in 1996.

Table 1. Signatures of plutonium isotopes for specific releases.

Captions corresponding with Fig. 1	**Origin of Pu**	**Activity ratio ^{238}Pu/$^{239+240}$Pu**	**Atomic ratio ^{240}Pu/^{239}Pu**
Global Fallout +SNAP 9A– Northern Hemisphere (1945-1980)		0.025 – 0.04 (Oughton et al., 2004)	0.175 – 0.19 (Oughton et al., 2004) 0.180 ± 0.014 (Kelley et al., 1999)
A	Thule (1968)	0.0150 ± 0.0017 (Mitchell et al., 1997)	0.033 ± 0.004 (Mitchell et al., 1997)
B	Palomares (1966)	0.0275 ± 0.0012 (Mitchell et al., 1997)	0.056 ± 0.003 (Mitchell et al., 1997)
C	High-yield thermonuclear explosions on Novaya Zemlya (1955-1962)	0.02 – 0.04 (Oughton et al., 2004)	0.16 – 0.20 (Oughton et al., 2004)
D	Chernobyl-fuel particles (1986)	0.45 – 0.52 (Kutkov et al., 1995)	0.186 – 0.348 (Ketterer et al., 2004)
E	Fukushima (2011)	1.1 – 2.9 (Zheng et al., 2013)	0.32 – 0.33 (Zheng et al., 2013)
F	Semipalatinsk-21 (1949-1961)	0.037 (Beasley et al., 1995)	0.0304 ± 0.0003 (Smith et al., 1995)
G	Lop Noir (1964-1974)	-	0.059 – 0.186 (Bu et al., 2015)
	Nagasaki atomic bomb (1945)	0.05 – 0.06 (Saito-Kokubu et al., 2008)	0.0283 ± 0.0002 (Saito-Kokubu et al., 2008)
H	Low yield detonations in the Nevada test site in USA (1951-1962)	-	0.032 ± 0.003 (Hicks and Barr, 1984)
	Weapons-grade plutonium	-	0.01 – 0.07 (Warneke et al., 2002)
Global Fallout +SNAP 9A-Southern Hemisphere (1951-1980)		0.14 (Hardy et al., 1973)	0.185 ± 0.047 (Kelley et al., 1999)
I	Ivy Mike (1952)	-	0.363 ± 0.004 (Hamilton, 2005)
J	Caste Bravo (1954)	-	0.32 ± 0.03 (Muramatsu et al., 2001)
K	French Polynesia (1966-1996)	-	0.04 (Bouisset et al., 2021)
L	Montebello (1956)	-	0.03 – 0.05 (Johansen et al., 2019)

2. Materials and methods

2.1 Sampling

Cryoconite was collected from cryoconite holes and deposits from the surface of 43 glaciers, providing 295 samples in total (Fig. 1, Supplementary Table S2). In addition, we consider published data from cryoconite sampled on a further seven glaciers (Baccolo et al., 2020; Buda et al., 2020; Łokas et al., 2022; Łokas et al., 2016; Łokas et al., 2019; Łokas et al., 2018). Overall, our data set includes 50 glaciers in the following macro-regions: Svalbard, the North American continent (including Greenland), the European sub-Arctic, Southern Europe, Asia, Africa, South America, the Antarctic Peninsula, and the McMurdo Dry Valleys in Antarctica. Details of the sampled glaciers and data from the literature are presented in Supplementary Table 1. For most glaciers, sampling was conducted within one season, although samples were collected over a longer period (> one year) for four glaciers (Gulkana; Urumqi No. 1; Suntarhyata No. 29-31; Exploradores). Cryoconite was sampled either with sterile disposable Pasteur pipettes or by scoops sterilized before taking each sample. Samples were placed in sterile vials, jars, or Whirl-Pak® bags. All sediment samples were either frozen as soon as possible after fieldwork or preserved in 70-96% ethyl alcohol.

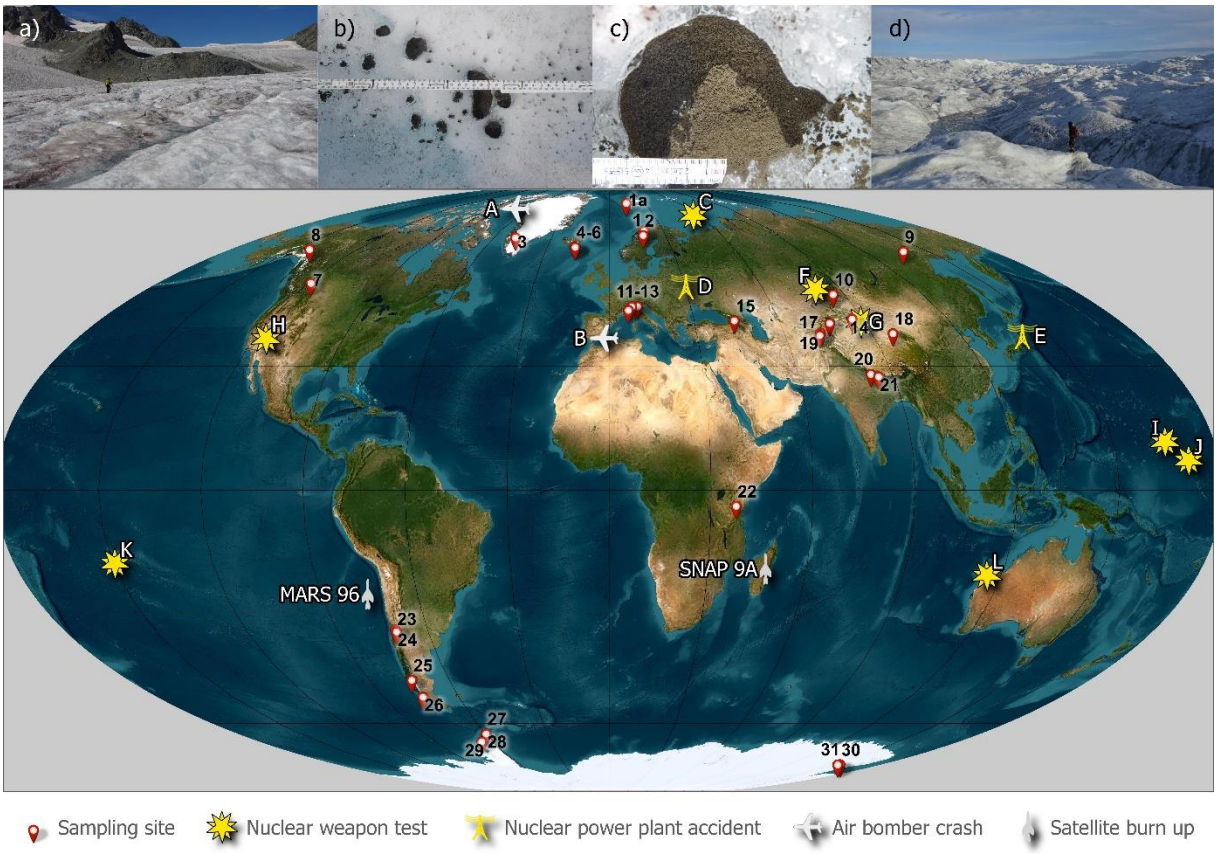

Inset panel a) depicts the surface of a mountain glacier with visible bedieres and likely ice algae bloom; b), c) show cryoconite holes with a thin layer of cryoconite sediment at the bottom; and panel d) shows the surface of the Greenland Ice Sheet.

Fig. 1. Sampling sites including the main nuclear tests (C, F, G, H, I, J, K, L), nuclear power plant accidents (D, E), air bomber crashes (A, B) and satellite burn-up events (SNAP 9A, MARS 96). Letters are defined in Table.1

Svalbard: **Svalbard:** 1a (11 glaciers) **Scandinavia:** 1. Steindalsbreen, 2. Isfallsglaciären; **Greenland:** 3. Russell Glacier; **Iceland:** 4. Skaftafellsjokull, 5. Virkisjokull, 6. Falljokull; **British Columbia, Canada**: 7. Castle Creek; **Alaska:** 8. Gulkana; **Asia:** 9. Suntarhyata Glacier No. 29-31, 10. Akkem Glacier, 14. Ürümqi No.1, 16. Grigoriev, 17. Lenin, 18. Qiyi, 19. Fedczenko, 20. Rhikasamba, 21. Yala; **the Alps:** 11. Zebrù, 12. Gries, 13. Tsanteleina; **Georgia:** 15. Gergeti Glacier; **Africa:** 22. Kersten Glacier; **South America:** 23. Iver, 24. El Morado, 25. Exploradores, 26. Tyndall; **South Shetland Islands:** 27. Ecology Glacier, 28. Baranowski, 29. Bonaparte; **McMurdo Dry Valleys:** 30. Canada, 31. Taylor.

2.2 Radiometric methods

The sampling procedure and radiochemical analysis of plutonium are described by Łokas et al. (Łokas et al., 2016; Łokas et al., 2018). All samples were nalysed and measured in the H. Niewodniczanski Institute of Nuclear Physics, Polish Academy of Sciences.

Samples were mineralized by ashing at 600 °C followed by wet digestion in concentrated HF, HNO_3, HCl and H_3BO_3. ^{242}Pu (Standard Reference Materials 4334j, NIST) was used as an internal tracer. Plutonium was separated on Dowex-1 from 8M HNO_3 after adjustment of the oxidation step as +4 using $H_4N_2 \cdot 2H_2O$ and $NaNO_2$ (LaRosa et al., 1992). Alpha spectrometric sources were prepared using the NdF_3 micro co-precipitation method (Sill, 1987). Finally, the alpha-spectrometric (AS) measurements were conducted using a PIPS® detector of 450 mm^2 active surface and Alpha Analyst™ 7200 spectrometer (Mirion Technologies). The typical counting time for each sample was 600,000 s. The data analysis was performed using Genie™ -2000 software (Mirion Technologies).

Uncertainties were calculated based on the error propagation law, and minimum detectable activity concentrations (MDC) were assessed using the Currie criterion (Currie, 1968). All activity concentrations and detection limits MDC refer to the dry mass of the sample. The mean activities and standard deviations for each geographic site (multiple samples were collected at each site) were also calculated.

2.3 Isotopic methods

After alpha-ray spectrometry measurements, all samples were prepared to determine the $^{240}Pu/^{239}Pu$ atom ratios using mass spectrometry. Sample preparation and detailed procedures are described in (Łokas et al., 2017) and summarized below. The membrane filters with plutonium isotopes deposited on their surface were dissolved using concentrated acids: HNO_3, H_3BO_3, HCl and $HClO_4$. Then, the Pu was adjusted to a +4 oxidation state, and a 3M HNO_3 feed solution was prepared. U and Th traces were purified on columns filled with TEVA resin (Triskem International). Thorium was removed with 9M HCl. The Pu fraction was eluted using 0.1M HCl and 0.1M HF. Traces of organic resin commonly present in the Pu eluate were

eliminated with the aid of concentrated $HClO_4$ and HNO_3. Pu salts were re-dissolved in 2% HNO_3 and 0.25% HF. Isotopic ratios were performed with the Agilent 8900#100 ICP-MS/MS (Agilent Technologies) coupled with Apex desolvating nebulizer (Elemental Scientific). The chemical recovery averaged at 70 ± 1% for Pu samples subjected to mass spectrometry. To reduce polyatomic interferences, Pu isotopes were measured in mass shift mode (+32 amu) using reaction with O_2 in collision reaction cell (CRC). Instrumental mass fractionation was monitored using IRMM-290 standard (EC, JRC) with certified $^{239}Pu/^{242}Pu$ atom ratios. External mass bias correction — determined applying the exponential law (Taylor et al., 2001) — was found negligible, usually less than 0.5%.

Data quality was evaluated through the preparation and analysis of IAEA Reference Materials (IAEA 447, IAEA 385) as well as blanks using the same analytical procedures. The results (Table 2) agreed well with recommended values and did not indicate any significant biases.

Table 2. Plutonium activities and isotope ratios in certified reference materials (CRM, IAEA) as analyzed in this study. The uncertainty is expressed as an expanded uncertainty using a level of confidence p = 95% (BIPM et al., 2008).

Reference material/standard (reference date)	$^{239+240}$Pu (Bq/kg)		^{238}Pu (Bq/kg)		$^{240}Pu/^{239}Pu$[1]	
	measured	certified	measured	certified	measured	certified
IAEA 385 (2019-01-01)	3.10 ± 0.30 (n = 5)	2.98 ± 0.25	0.438 ± 0.040 (n = 5)	0.392 ± 0.021	0.1771 ± 0.0019 (n = 5)	0.174 ± 0.031 (Pham et al., 2008)
IAEA 447 (2021-03-01)	5.008 ± 0.087 (n = 3)	5.30 ± 0.31	0.141 ± 0.020 (n = 3)	0.150 ± 0.039	0.1869 ± 0.0022 (n = 9)	0.186 ± 0.022 (Bu et al., 2013)

[1]atom ratio

2.4 Parametrization of environmental characteristics

The organic matter (OM) content of cryoconite was measured as a percentage weight loss through combustion at 600 °C for 6 h. Data on organic matter are presented for cryoconite samples from all glaciers (Table S2). To understand whether precipitation affected activity concentrations of $^{239+240}$Pu deposition during the maximum nuclear weapon tests (peak in 1963), we calculated the sum of precipitation in each considered region from January 1962 to December 1964, using the WorldClim v2.1 (Fick and Hijmans, 2017; Harris et al., 2020) database with 2.5-min (latitude and longitude) spatial resolution. These data do not cover the Antarctic region, so glaciers from this region were excluded from this analysis. Each glacier

was also characterised as either valley or outlet-type, and the mean altitude of each glacier was identified (Table S2).

2.5 Statistical analysis

To test whether the activity concentration of plutonium isotopes is related to environmental characteristics (i.e., mean organic matter content of cryoconite, regional precipitation (only for $^{239+240}$Pu activity concentration analysis), altitude, glacier type), we built a Linear Mixed Models (LMM). We built separate full models for ^{238}Pu and $^{239+240}$Pu as response variables (mean value for each glacier) which were log-transformed to reduce the effect of influential observations. Moreover models included the above set of predictors as additive fixed effects, and macro-region as random intercept effects (n = 9). Such model structure enables us to control unknown variations between macro-regions. We also built models that included organic matter as a random slope effect, however, the amount of variance explained by it was minor, therefore we report models with random intercept only. We selected the best models from the pool of possible models containing all combinations of fixed effects based on the Akaike Information Criterion for small sample sizes (AICc). The models were estimated for 29 glaciers that have a complete dataset. Full models were fitted using Maximum Likelihood estimation, after model selection using the MuMIn package (Barton, 2009), and the chosen models were then re-estimated using the Restricted Maximum Likelihood approach.

We compared the activity concentrations and ratios between hemispheres using two-sample Wilcoxon (W) tests. To analyze the multiple comparisons between plutonium isotopes' activities and ratios between regions, we employed the Kruskal-Wallis test with Dunn's posthoc tests, applying a Benjamini-Hochberg adjustment to the p-values (Benjamini and Hochberg, 1995). None of the comparisons met the assumptions for parametric testing.

Models were estimated in R 3.6.3 software (R Core Team 2022) using the glmmTMB package (Brooks et al., 2017) and checked for any violation of assumptions based on diagnostic plots. Data with the commented R-code are deposited under the link: https://github.com/jakbud1/Isotopic-signature-of-plutonium-accumulated-in-glaciers-worldwide.git

3. Results & discussion

3.1 Plutonium levels in cryoconite

Figures 2 and 3 present the global variation of $^{239+240}$Pu and ^{238}Pu activity concentrations along with organic matter content based on the results of this study and on previously published data

(Table S1). The average $^{239+240}$Pu activity concentration per glacier was significantly higher in the Northern Hemisphere (mean = 21.84 Bq kg^{-1}, SE = 5.38; median = 8.72 Bq kg^{-1}; IQR = 20.33) than the Southern Hemisphere (mean = 5.38 Bq kg^{-1}, SE = 2.15; median = 5.15 Bq kg^{-1}; IQR = 4.98) (Z = 1.992, P = 0.047; Fig. 2a, b). The highest activity concentrations of $^{239+240}$Pu for individual samples exceeded 179 Bq kg^{-1} and were found in cryoconite from the Werenskiold Glacier in the Svalbard Archipelago (Fig. 2). Among the mainland European glaciers, the highest value of $^{239+240}$Pu (110 Bq kg^{-1}) was found in cryoconite from the Zebrù Glacier (Italian Alps). Activity concentrations of $^{239+240}$Pu varied significantly between macro-regions (Kruskal-Wallis χ^2 = 44.93, df = 7, $p < 0.001$) with a general pattern of European sub-Arctic and southern European sites being more contaminated than other macro-regions (Fig. 2, Supplementary Table S2). Lower but still elevated activity concentrations (> 65 Bq kg^{-1}) were recorded for Tienshan and Suntar-Khayata (Asia) glaciers. In all samples from Kersten Glacier on Kilimanjaro, plutonium activity concentrations were below the detection limit (< 0.050 Bq kg^{-1}). In the Southern Hemisphere, the highest value was observed for the Exploradores Glacier (18 Bq kg^{-1}) at 250 m a.s.l and Bonaparte Point (16 Bq kg^{-1}) in King George Island. The lowest values of $^{239+240}$Pu were observed in McMurdo Dry Valleys in Antarctica (Fig. 2).

Activity concentrations of ^{238}Pu revealed no differences between hemispheres (Z = 0.125, p = 0.928; Fig. 3a, b). However, similarly to $^{239+240}$Pu, some regional variation was found (Kruskal-Wallis χ^2 = 35.74, df = 7, $p < 0.001$; Fig. 3), showing a general trend of European Subarctic sites being more contaminated by ^{238}Pu than other macro-regions (Fig. 3, Supplementary Table S3). The highest activity concentrations of ^{238}Pu were found in both hemispheres on the glaciers with the highest activity concetrations of $^{239+240}$Pu (Werenskiold Glacier, 13.14 Bq k g^{-1}; Exploradores Glacier, 7.22 Bq kg^{-1}). The lowest values were measured in the Taylor and Canada Glaciers located in the McMurdo Dry Valleys of Antarctica (Victoria Land, Ross Sea region).

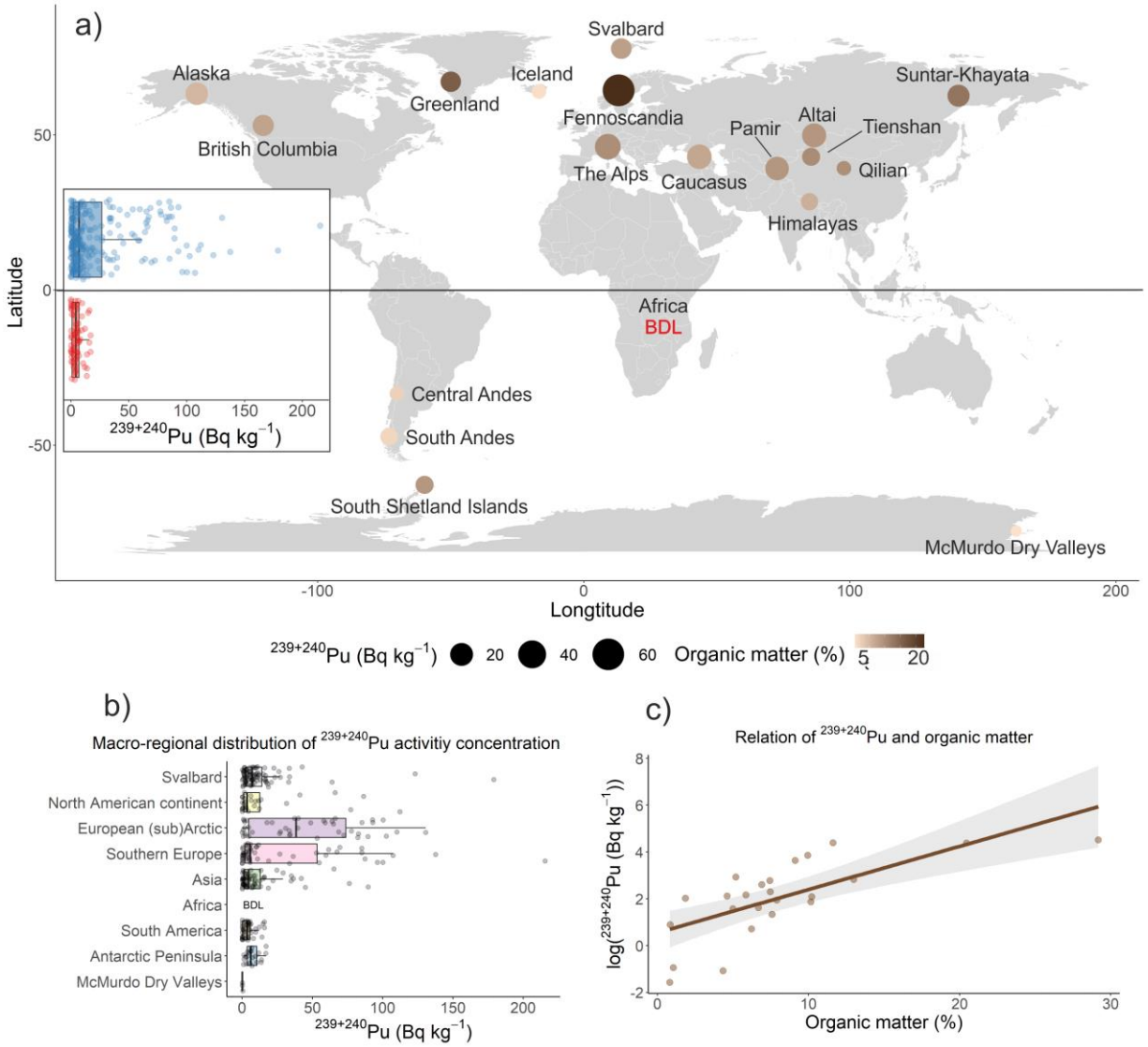

Figure 2. Global distribution of $^{239+240}$Pu in cryoconite on glaciers. **a)** Map illustrating activity concentrations and organic matter content at a regional scale; the insert on the map displays the variation in $^{239+240}$Pu activity concentration between hemispheres. **B)** Macro-regional variation in $^{239+240}$Pu activity concentrations. **C)** Relation between $^{239+240}$Pu activity concentration and organic matter content in cryoconite; partial residuals of Linear Mixed Models with macro-region as a random intercept effect. BDL – below detection limit; the mean organic matter content for Africa (Kersten glacier) is 3.22%.

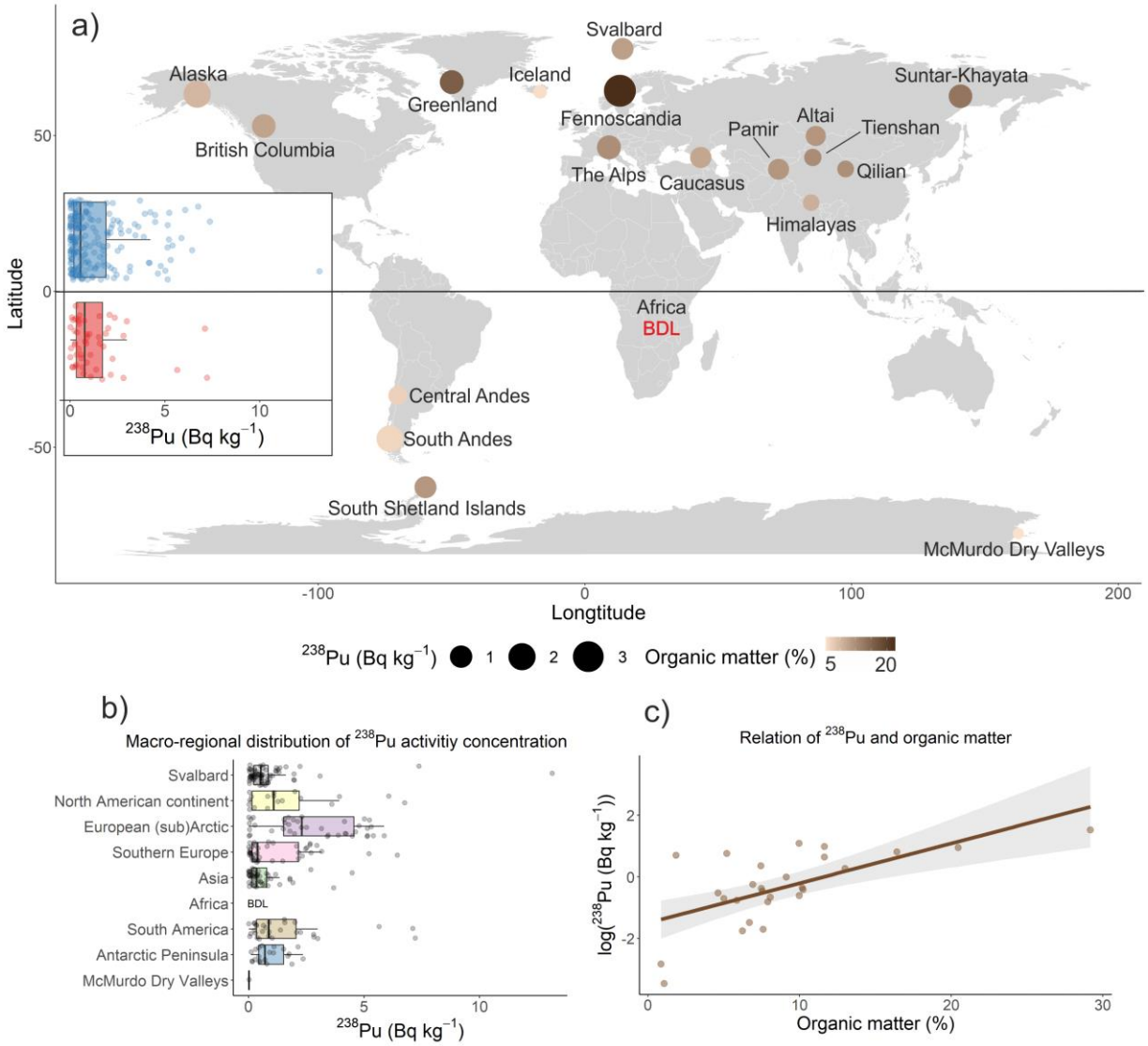

Figure 3. Global distribution of ^{238}Pu in cryoconite on glaciers. **A)** Map illustrating activity concentration and organic matter content at a regional scale; the insert on the map illustrates the variation in ^{238}Pu activity concentrations between hemispheres. **B)** Macro-regional variation in ^{238}Pu activity concentrations. **C)** Relationship between ^{238}Pu activity concentration and organic matter content in cryoconite; partial residuals of Linear Mixed Models with macro-region as a random intercept effect. BDL – below detection limit; the mean organic matter content for Africa (Kersten Glacier) is 3.22%.

3.2 Factors affecting Pu activity concentrations

Of all variables considered here, organic matter content is the only significant predictor for activity concentrations of $^{239+240}$Pu ($\chi^2 = 29.74$, df = 1, $p < 0.001$) and ^{238}Pu ($\chi^2 = 16.05$, df = 1, $p < 0.001$) on the global scale. In both cases, Pu isotope activity concentration (log-scaled) increases with cryoconite organic matter content (Figs 2c and 3c). Glacier elevation, glacier

type (valley vs outlet) or the sum of precipitation during the peak period of global fallout do not have a significant effect on activity concentrations with macro-region included as a random effect. However, for individual glaciers we observed various types of relationships between organic matter content and Pu isotopes activity concentrations (Figs S1 and S2), from negative correlation (Spearman-rank correlation = -0.44; El Morado Glacier), through no correlation (e.g, Spearman-rank correlation = 0.04; Renardbreen Glacier) to a positive correlation (e.g. Spearman-rank correlation = 0.93; Gries Glacier). The above examples are for $^{239+240}$Pu, while the trend is similar for ^{238}Pu. However, we point out that lack of correlation might be due to low sample sizes for some glaciers (Fig. S1 and S2). Therefore, the intra-glacier relationships should be treated carefully, particularly as the primary purpose of this work was to conduct a global and regional comparison. Our results are generally consistent with previous studies (e.g.(Baccolo et al., 2020; Buda et al., 2023; Clason et al., 2023; Łokas et al., 2022) highlighting the role of organic matter in the accumulation of legacy pollutants in cryoconite on glaciers worldwide.

3.3 Global isotopic composition of plutonium in the Northern and Southern Hemispheres

The ^{238}Pu/$^{239+240}$Pu isotope ratios in cryoconite samples collected from the Northern and Southern Hemispheres varied from 0.004 ± 0.002 to 0.089 ± 0.003 and from 0.041 ± 0.022 to 0.590 ± 0.056, respectively. The ratio for the Northern Hemisphere (median = 0.054; IQR = 0.023) was lower ($Z = -3.308$, $p < 0.001$; Fig. 4a,c) than for the Southern Hemipshere (median = 0.119; IQR = 0.047). The ^{240}Pu/^{239}Pu mass ratios varied from 0.089 ± 0.003 to 0.217 ± 0.080 in the Northern Hemisphere, and from 0.038 ± 0.003 to 0.245 ± 0.020 in the Southern Hemisphere. The ratio was higher ($Z = 2.853$, $p = 0.003$; Fig. 4b,d) for the Nothern Hemisphere (median = 0.159; IQR = 0.022) than for the Southern Hemisphere (median = 0.098; IQR = 0.038, Table S2). Relatively high variability in both ratios was found for the Southern Hemisphere, especially in South America (Fig 4a, b). The highest isotopic ratios in the Northern Hemisphere were observed in the North American continent, especially in British Columbia, Canada, and Greenland, but the lowest value was observed in Iceland, which belongs to the same macro-region. Sources of radionuclides in the Southern Hemisphere are more limited – including the tests conducted by France, the UK and the USA – and are characterized by the lack of significant fallout in this hemisphere. A wide range of Pu ratios was also observed by Szufa et al. (2018) in marine organisms from the South Shetland Islands, where the water

masses are characterized by diverse isotopic ratios and where marine organisms are exposed to plutonium with isotopic ratios different than in other parts of the world.

The $^{240}Pu/^{239}Pu$ ratios in Northern Hemisphere cryoconite (0.154 ± 0.026) are generally comparable to or slightly lower (Fig. 4b, c) than the values of 0.180 ± 0.014 (Kelley et al., 1999; Krey et al., 1976) or 0.173 ± 0.027 (Koide et al., 1985) reported for the integrated atmospheric global fallout. Cryoconite samples only exhibit a lower $^{240}Pu/^{239}Pu$ mass ratio in British Columbia and Alaska, ranging from 0.090 to 0.175. This is probably due to the contribution from the Nevada Test Site fallout characterized by the average $^{240}Pu/^{239}Pu$ ratio of 0.03 (Hicks and Barr, 1984). The Southern Hemisphere regions, on the other hand, have received a mix of tropospheric and stratospheric debris from the USA and UK Pacific Proving Ground (PPG) tests, and French tests at Mururoa and Fangataufa Atolls (Krey et al., 1976). Significant tropospheric debris is present in the Southern Hemisphere because of a high tropopause height at latitudes encompassing PPG and French test sites (Alvarado et al., 2022). Moreover, PPG tests were typically surface tests of varying yields and types that generated large amounts of tropospheric debris (US Department of Energy, 1988).

The $^{240}Pu/^{239}Pu$ mass ratios collected on Kersten Glacier on Kilimanjaro, Tanzania (0.145-0.176) were lower than those observed in soils from Central Africa (e.g., Mozambique, Kenya, Angola) where the $^{240}Pu/^{239}Pu$ ratio varied between 0.174 to 0.190 (Kelley et al., 1999). This discrepancy could be explained by a contribution of fallout from some regional source, similarly to the presumed contribution from the Nevada Test Site to British Columbian and Alaskan glaciers. However, in this case, we hypothesize that the source of low $^{240}Pu/^{239}Pu$ contamination is associated with French nuclear weapons test in the Pacific Ocean (0.04) (Bouisset et al., 2021; Chaboche et al., 2022). The $^{240}Pu/^{239}Pu$ mass ratios in cryoconite collected from the South Shetland Islands varied between 0.098 and 0.209. However, for samples collected in the McMurdo Dry Valleys ratios ranging between 0.202 to 0.245 were found (Table S2). The South Shetland Islands samples might correspond to a mix of fallout originating from global fallout (0.173 ± 0.027) and weapons-grade Pu with a ratio lower than 0.07. The higher $^{240}Pu/^{239}Pu$ mass ratios measured in the McMurdo Dry Valleys are comparable to the value of 0.276 ± 0.011 reported for soil in Rongelap Atoll (Muramatsu et al., 2001) or to the value of 0.25 ± 0.01 reported for soils from Bikar atoll, northern Marshall Islands (Alvarado et al., 2022). This suggests that the Pu contamination in Rongelap, Bikar and the McMurdo Dry Valleys is dominated by the contamination produced by the Castle Bravo test in 1954 in Bikini (Lachner et al., 2010; Muramatsu et al., 2001).

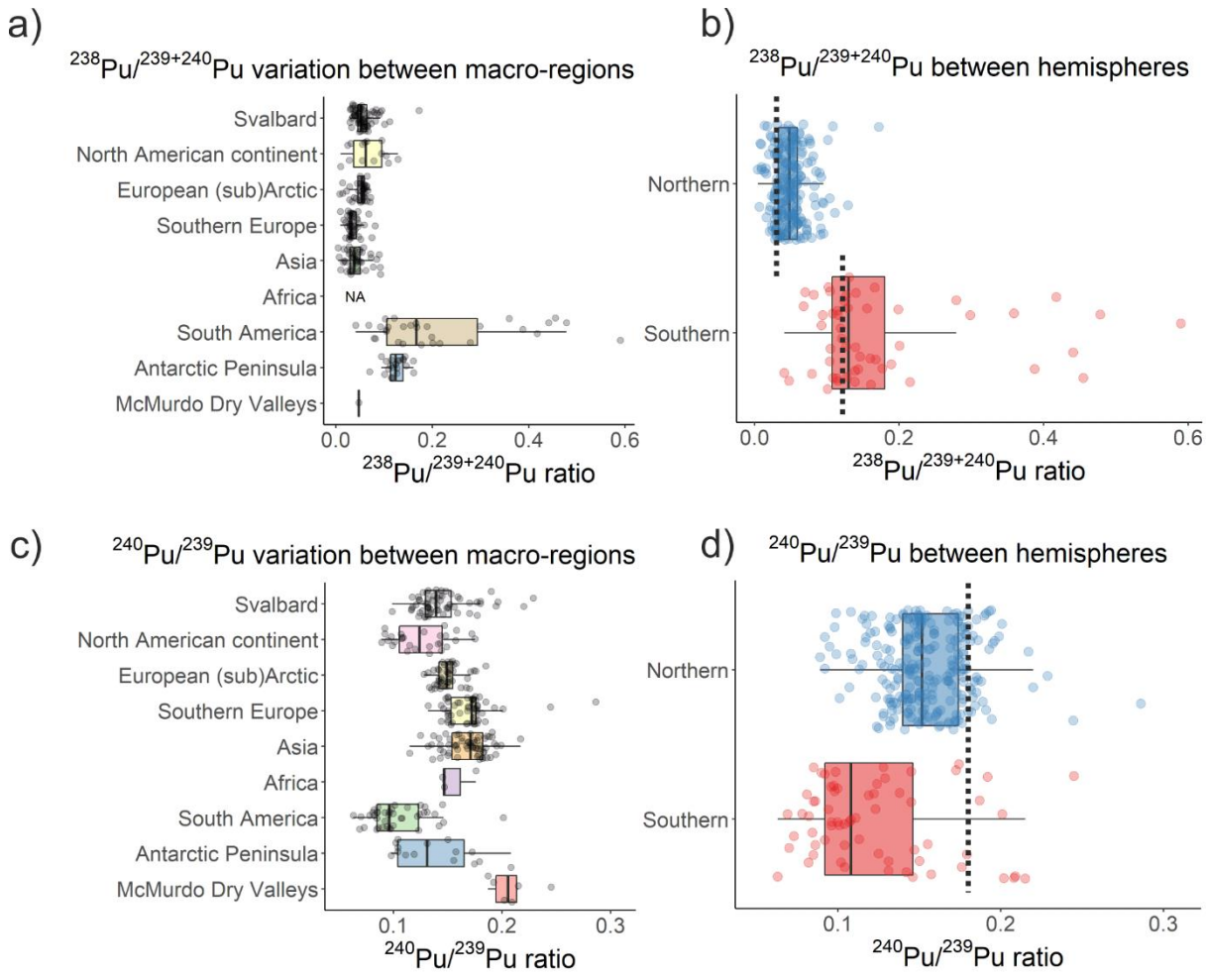

Figure 4. Global distribution of activity ($^{238}Pu/^{239+240}Pu$) and atomic ($^{240}Pu/^{239}Pu$) ratios in cryoconite on glaciers. **a)** Macro-regional variation in $^{238}Pu/^{239+240}Pu$ activity ratios. **b)** Comparison of $^{238}Pu/^{239+240}Pu$ between hemispheres, dotted lines: 0.03 and 0.13 corresponds to the global fallout with SNAP 9A in the Northern and Southern Hemispheres, respectively. **c)** Macro-regional variation in $^{240}Pu/^{239}Pu$ activity ratios. **d)** Comparison of $^{240}Pu/^{239}Pu$ between hemispheres, dotted line: 0.18 corresponds to the global fallout in the Northern and Southern Hemisphers.

3.4 Isotopic composition of plutonium on glaciers in South America

The origin of plutonium in South America is discussed separately due to the characteristic values of Pu ratios found there. Four glaciers were investigated in South America: Exploradores and Tyndal glaciers (Southern Andes, Fig. 1), which are relatively low-lying with elevations up to 700 m a.s.l.; and El Morado and Iver glaciers (Central Andes, Fig. 1) with elevations up to 4400 m a.s.l. Exporadores and Tyndall are large glacier that drain the Northern and the Southern Patagonian Ice Fields respectively (Takeuchi and Kohshima, 2004). They lie in a remote area, and their tongues are at low elevation, with the tongue of Exploradores reaching a relatively

warm coastal area. Iver and El Morado are two small glaciers close to Santiago de Chile. Iver is particularly exposed to pollutants from urban areas (Pittino et al., 2023).

The Pu in the Southern Hemisphere is assumed to be a mixture of global fallout and SNAP fuel with a $^{238}Pu/^{239+240}Pu$ ratio of 0.20 (0.13 decay corrected for 2023) and 0.18 (0.12 decay corrected for 2023) in the latitude bands 20 – 30°S and 30 – 40°S, respectively, showing the significant impact of the satellite failure (Hardy et al., 1973). The ratios found for Tyndall and El Morado glaciers agree with the above signatures, while the $^{238}Pu/^{239+240}Pu$ ratios found for Exploradores glacier were significantly higher (Fig. 5c).

Samples from Exploradores glacier were collected in 2018 and 2019 from approximately the same area in both years. Ablation is intense on this glacier, and cryoconite holes do not last for many days. No physical differences were observed between the characteristics of holes and cryoconite sediment in these two field campaigns. However, ^{238}Pu activity concentrations and $^{238}Pu/^{239+240}Pu$ isotopic ratios varied considerably from 1.397 ± 0.111 Bq kg^{-1} to 18.007 ± 1.328 Bq kg^{-1} and 0.102 ± 0.018 to 0.479 ± 0.052, respectively (Fig. 5a, c; Table S2 Excel). According to the IAEA report (Radiation and Safety, 2001), the signature of samples showing such a high contribution from ^{238}Pu cannot be explained by Pu sources traditionally used to explain the typical Pu isotopic variability found in the environment. Other events must thus be considered. One of those events is the atmospheric re-entry of the automatic Interplanetary Station "Mars '96" which occurred on November 17, the day after the spacecraft was launched. The crash site is not known, but it is estimated to be in a 320 km by 80 km area which includes parts of the Pacific Ocean, Chile, and Bolivia. No traces of the crash have been found and no information is available about the exact site (Galeev, 1996). There were considerable quantities of ^{238}Pu on board the spacecraft, with a total activity of 174 TBq. Elevated $^{238}Pu/^{239+240}Pu$ (up to 0.283 ± 0.029) activity ratios were also observed in peat samples from Madagascar by Raaf et al. (Rääf et al., 2017) and in soils from Mozambique (up to 0.235) (Hardy et al., 1973). As a further comparison, values of ~0.25 and 0.27 have been reported for Antarctic lichens and mosses (Roos et al., 1994; Szufa et al., 2018).

The cryoconite samples from South America (Exloradores, Tyndall, and El Morado glaciers) exhibit $^{240}Pu/^{239}Pu$ mass ratios (Fig. 6) that differ significantly from the average value of 0.180 ± 0.014 reported for the integrated atmospheric global fallout (Kelley et al., 1999; Krey et al., 1976) or 0.173 ± 0.027 (Koide et al., 1985), however, they are comparable to the typical ratio of < 0.07 reported for weapons-grade Pu. The average Pu mass ratio is 0.094 ± 0.010 for Exploradores, 0.071 ± 0.019 for El Morado, and 0.091 ± 0.031 for Tyndal. Iver glacier was characterized by the highest average $^{240}Pu/^{239}Pu$ mass ratio of 0.138 ± 0.023. Atmospheric

transport of plutonium via sea-salt aerosols is another potential source of plutonium in glaciers close to the sea (e.g. (Cambray and Eakins, 1982)). All samples from the Andes and South Shetland Islands have $^{240}Pu/^{239}Pu$ ratios in a wide range reflecting mixing of weapons-grade Pu and global fallout in different proportions (Fig. 6). A similar range of $^{240}Pu/^{239}Pu$ atomic ratios was found by (Chamizo et al., 2011) in soil samples from the 20 – 40°S latitude band in Chile. The lowest ratios might reflect the contribution of plutonium released in the low-yield tests performed in Montebello and French Polynesia (Table 1). This hypothesis can be supported by documents and maps published by the French Ministry of Defence in 2013 and (Cai et al., 2020) regarding the spatial extent and dominant circulation from west to east of radiactive clouds released from nuclear test conducted by France in 1967 and 1968. The highest ratios were found for El Morado and Iver glaciers located in the dry Andes at high eleveations (3300 and 4400 m a.s.l) where the deposition of tropospheric debris from nuclear tests might have been enhanced. Most of these tests were conducted hundreds of meters above sea level, so the corresponding fallout, mostly of fine-grained particles, may have travelled thousands of kilometres in the troposphere. South of 40 °S the $^{240}Pu/^{239}Pu$ atomic ratios show an increasing trend with latitude, reaching 0.245 in Canada glacier (McMurdo Dry Valleys).

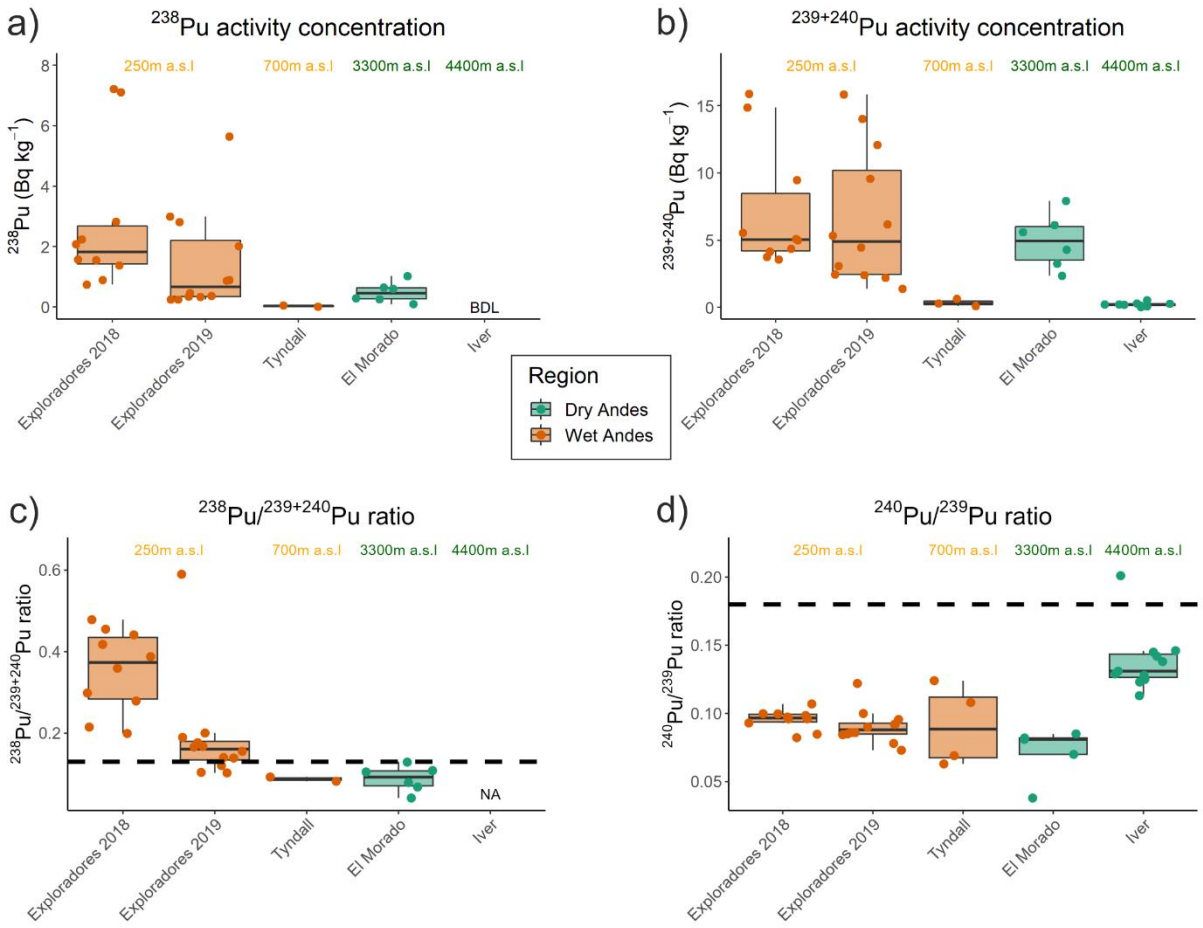

437

438 **Figure 5.** Distribution of activity concentrations as well as activity and atomic ratios of plutonium isotopes in
439 cryoconite on glaciers in South America. **a)** ^{238}Pu activity concentrations, **b)** $^{239+240}$Pu activity
440 concentrations, **c)** ^{238}Pu/$^{239+240}$Pu activity ratios, dotted line: 0.13 corresponds to the global fallout with
441 SNAP 9A in the Southern Hemisphere. **d)** ^{240}Pu/^{239}Pu atomic ratios, dotted line: 0.18 corresponds to the
442 global fallout in the Southern Hemisphere.

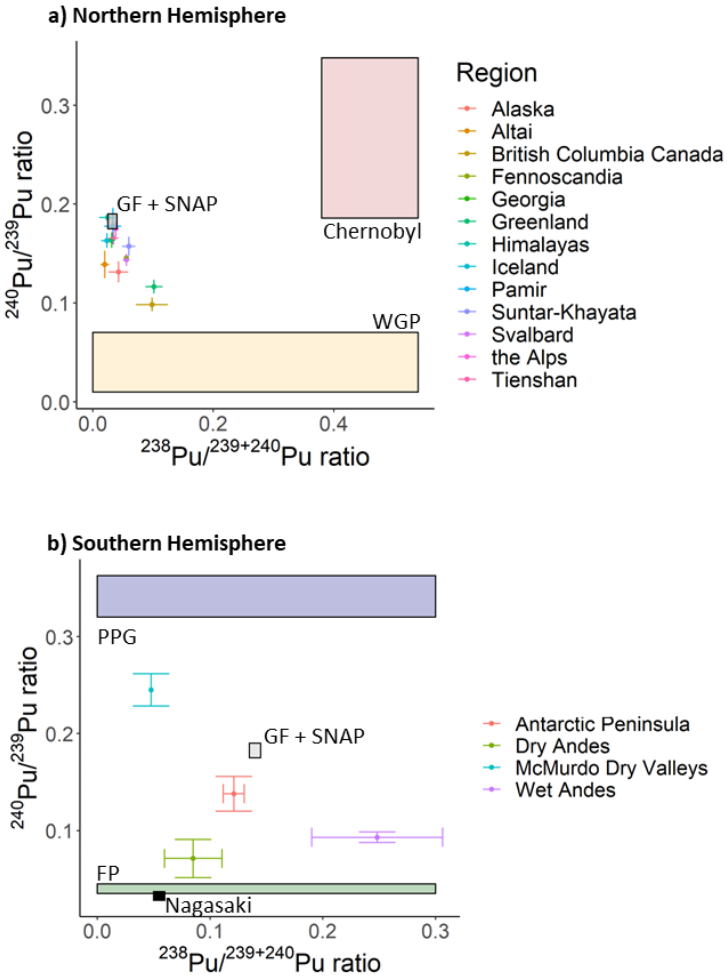

Figure 6. Range of $^{240}Pu/^{239}Pu$ and $^{238}Pu/^{239+240}Pu$ ratios on a regional scale for both hemispheres. Dots represent the means for each region while whiskers are 95% CIs of the mean. Rectangles cover ratios in ranges of specific sources: GF – Global Fallout, SNAP – SNAP 9A satellite burn-up, WGP – Weapons-Grade Plutonium, PPG - Pacific Proving Grounds nuclear weapon tests, FP – French Polynesia nuclear weapon tests (Table 1).

4 Conclusions

This study provides new insights into the provenance of Pu isotopes (^{238}Pu, ^{239}Pu, ^{240}Pu) in glaciers based on cryoconite samples collected from nine glaciated regions of six continents. The $^{239+240}Pu$ activity concentrations are significantly higher in the Northern Hemisphere than the Southern Hemisphere which reflects the uneven deposition of global fallout between

hemispheres. Within the Northern Hemisphere the highest concentrations occur in Scandinavia and in the European Alps. Unlike $^{239+240}$Pu, there is no significant difference in ^{238}Pu activity concentrations between the hemispheres. Cryoconite from the Southern Hemisphere is characterized by large heterogeneity with respect to both the activity and mass ratios. The relative enrichment in ^{238}Pu observed in cryoconite from the Southern Hemisphere is partly due to the recognized contribution of the re-entry of the SNAP satellite. Nevertheless, our results show that some regions of the Southern Hemsphere received ^{238}Pu from other non-global sources, in particular South America. We suggest as potential candidates, the failure of the Mars '96 probe or low-yield nuclear weapons testing in the Southern Pacific. Further analyses are needed to constrain our hypotheses, possibly involving sediments from that region providing a resolvable depositional isotopic history.

The activity and mass ratios of plutonium in cryoconite reflect contributions from regional-scale contamination, signals that may be lost in soils and other environmental archives of atmospheric radionuclide deposition. Cryoconite thus represents an important, and largely ignored, environmental material for the mapping of the deposition of plutonium from the past as well as from future releases.

Acknowledgements

This study was supported by the National Science Center grant no. NCN 2018/31/B/ST10/03057 (PI: Edyta Łokas). Sample collection in Sweden and Iceland was funded by INTERACT Transnational Access and QRA grants, respectively, awarded to Caroline Clason. We thank the CONAF (Corporación Nacional Forestal of Chile) for the permission and support in collecting supraglacial samples on the Exploradores Glacier.

Author contributions:

Conceptualization: EŁ, GB, PW, JB, CC, PNO

Sample collection: NT, GB, BDM, CC, KZ, RA, FP

Methodology and Analysis: EŁ, AC, KK

Interpretation of data: EŁ, AC, KK, JB

Visualization of data: JB, AC

Writing—original draft: EŁ, JB, PW, GB, RA, DBB, CC, PNO, KZ

Writing—review & editing: EŁ, GB, PW, JB, CC, PNO, RA, NT, FP, AF, MN, MS, BDM

Supervision and funding acquisition: EŁ

References

Alvarado, J.C., Röllin, S., Sahli, H., McGinnity, P. (2022) Isotopic signatures of plutonium and uranium at Bikar atoll, northern Marshall Islands. Journal of Environmental Radioactivity 242, 106795.
Baccolo, G., Łokas, E., Gaca, P., Massabò, D., Ambrosini, R., Azzoni, R.S., Clason, C., Di Mauro, B., Franzetti, A., Nastasi, M. (2020) Cryoconite: an efficient accumulator of radioactive fallout in glacial environments. The Cryosphere 14, 657-672.
Barton, K. (2009) MuMIn: multi-model inference. http://r-forge. r-project. org/projects/mumin/.
Beasley, T., Cooper, L., Grebmaier, J., Orlandini, K., Kelley, J. (1995) Fuel reprocessing Pu in the Arctic Ocean basin. Evidence from mass spectrometry measurements.
Benjamini, Y., Hochberg, Y. (1995) Controlling the false discovery rate: a practical and powerful approach to multiple testing. Journal of the Royal statistical society: series B (Methodological) 57, 289-300.
BIPM, I., IFCC, I., ISO, I., IUPAP, O. (2008) Evaluation of measurement data—Guide to the expression of uncertainty in measurement. Joint Committee for Guides in Metrology, JCGM 100: 2008. Citado en las, 18-21.
Bouisset, P., Nohl, M., Cossonnet, C., Boulet, B., Thomas, S., Cariou, N., Salaun, G. (2021) Contribution of close-in fallout from the French atmospheric tests in inventories of 137Cs, 241Am and plutonium (238, 239, 240) in Gambier Islands (French Polynesia)–Signatures of stratospheric fallout in the Southern Hemisphere. Journal of Environmental Radioactivity 235, 106624.
Brooks, M.E., Kristensen, K., Van Benthem, K.J., Magnusson, A., Berg, C.W., Nielsen, A., Skaug, H.J., Machler, M., Bolker, B.M. (2017) glmmTMB balances speed and flexibility among packages for zero-inflated generalized linear mixed modeling. The R journal 9, 378-400.
Bu, K., Cizdziel, J.V., Dasher, D. (2013) Plutonium concentration and 240Pu/239Pu atom ratio in biota collected from Amchitka Island, Alaska: recent measurements using ICP-SFMS. Journal of environmental radioactivity 124, 29-36.
Bu, W., Ni, Y., Guo, Q., Zheng, J., Uchida, S. (2015) Pu isotopes in soils collected downwind from Lop Nor: regional fallout vs. global fallout. Scientific reports 5, 12262.
Buda, J., Łokas, E., Błażej, S., Gorzkiewicz, K., Buda, K., Ambrosini, R., Franzetti, A., Pittino, F., Crosta, A., Klimaszyk, P. (2023) Unveiling threats to glacier biota: Bioaccumulation, mobility, and interactions of radioisotopes with key biological components. Chemosphere, 140738.
Buda, J., Łokas, E., Pietryka, M., Richter, D., Magowski, W., Iakovenko, N.S., Porazinska, D.L., Budzik, T., Grabiec, M., Grzesiak, J. (2020) Biotope and biocenosis of cryoconite hole ecosystems on Ecology Glacier in the maritime Antarctic. Science of the Total Environment 724, 138112.
Cai, W., McPhaden, M.J., Grimm, A.M., Rodrigues, R.R., Taschetto, A.S., Garreaud, R.D., Dewitte, B., Poveda, G., Ham, Y.-G., Santoso, A. (2020) Climate impacts of the El Niño–southern oscillation on South America. Nature Reviews Earth & Environment 1, 215-231.
Cambray, R., Eakins, J. (1982) Pu, 241Am and 137Cs in soil in West Cumbria and a maritime effect. Nature 300, 46-48.
Chaboche, P.-A., Pointurier, F., Sabatier, P., Foucher, A., Tiecher, T., Minella, J.P., Tassano, M., Hubert, A., Morera, S., Guédron, S. (2022) 240Pu/239Pu signatures allow refining the chronology of radionuclide fallout in South America. Science of the Total Environment 843, 156943.
Chamizo, E., García-León, M., Peruchena, J., Cereceda, F., Vidal, V., Pinilla, E., Miró, C. (2011) Presence of plutonium isotopes, 239Pu and 240Pu, in soils from Chile. Nuclear Instruments and Methods in Physics Research Section B: Beam Interactions with Materials and Atoms 269, 3163-3166.
Clark, D.L., Geeson, D.A., Hanrahan, R.J. (2019) Plutonium handbook. American Nuclear Sociedty.

Clason, C.C., Baccolo, G., Łokas, E., Owens, P.N., Wachniew, P., Millward, G.E., Taylor, A., Blake, W.H., Beard, D.B., Poniecka, E. (2023) Global variability and controls on the accumulation of fallout radionuclides in cryoconite. Science of the Total Environment, 164902.
Clason, C.C., Blake, W.H., Selmes, N., Taylor, A., Boeckx, P., Kitch, J., Mills, S.C., Baccolo, G., Millward, G.E. (2021) Accumulation of legacy fallout radionuclides in cryoconite on Isfallsglaciären (Arctic Sweden) and their downstream spatial distribution. The Cryosphere 15, 5151-5168.
Cook, J., Edwards, A., Takeuchi, N., Irvine-Fynn, T. (2016) Cryoconite: the dark biological secret of the cryosphere. Progress in Physical Geography 40, 66-111.
Currie, L.A. (1968) Limits for qualitative detection and quantitative determination. Application to radiochemistry. Analytical chemistry 40, 586-593.
Di Mauro, B., Baccolo, G., Garzonio, R., Giardino, C., Massabò, D., Piazzalunga, A., Rossini, M., Colombo, R. (2017) Impact of impurities and cryoconite on the optical properties of the Morteratsch Glacier (Swiss Alps). The Cryosphere 11, 2393-2409.
Engelbrecht, R., Schwaiger, M. (2008) State of the art of standard methods used for environmental radioactivity monitoring. Appl. Rad. Isotop. 66, 1604-1610.
Fick, S.E., Hijmans, R.J. (2017) WorldClim 2: new 1-km spatial resolution climate surfaces for global land areas. International journal of climatology 37, 4302-4315.
Gabrieli, J., Cozzi, G., Vallelonga, P., Schwikowski, M., Sigl, M., Eickenberg, J., Wacker, L., Boutron, C., Gäggeler, H., Cescon, P. (2011) Contamination of Alpine snow and ice at Colle Gnifetti, Swiss/Italian Alps, from nuclear weapons tests. Atmospheric Environment 45, 587-593.
Galeev, A. (1996) Russian program of planetary missions. Acta astronautica 39, 9-14.
Hamilton, T.F., (2005) Linking legacies of the cold war to arrival of anthropogenic radionuclides in the oceans through the 20th century, Radioactivity in the Environment. Elsevier, pp. 23-78.
Hardy, E., Krey, P., Volchok, H., (1972) PLUTONIUM FALLOUT IN UTAH.
Hardy, E., Krey, P., Volchok, H. (1973) Global inventory and distribution of fallout plutonium. Nature 241, 444-445.
Harris, I., Osborn, T.J., Jones, P., Lister, D. (2020) Version 4 of the CRU TS monthly high-resolution gridded multivariate climate dataset. Scientific data 7, 109.
Hicks, H., Barr, D. (1984) Nevada test site fallout atom ratios: 240Pu/239Pu and 241Pu/239Pu.
Jaworowski, Z., Kownacka, L., Grotowski, K., Kwiatkowski, K. (1978) Lead-210 from nuclear explosions in the environment. Nuclear Technology 37, 159-166.
Johansen, M., Child, D., Cresswell, T., Harrison, J., Hotchkis, M., Howell, N., Johansen, A., Sdraulig, S., Thiruvoth, S., Young, E. (2019) Plutonium and other radionuclides persist across marine-to-terrestrial ecotopes in the Montebello Islands sixty years after nuclear tests. Science of the total environment 691, 572-583.
Kelley, J., Bond, L., Beasley, T. (1999) Global distribution of Pu isotopes and 237Np. Science of the Total Environment 237, 483-500.
Ketterer, M.E., Hafer, K.M., Mietelski, J.W. (2004) Resolving Chernobyl vs. global fallout contributions in soils from Poland using Plutonium atom ratios measured by inductively coupled plasma mass spectrometry. Journal of Environmental Radioactivity 73, 183-201.
Koide, M., Bertine, K.K., Chow, T.J., Goldberg, E.D. (1985) The240Pu239Pu ratio, a potential geochronometer. Earth and planetary science letters 72, 1-8.
Krey, P., Hardy, E., Pachucki, C., Rourke, F., Coluzza, J., Benson, W., (1976) Mass isotopic composition of global fall-out plutonium in soil, Transuranium nuclides in the environment.
Krey, P., Leifer, R., Benson, W., Dietz, L., Hendrikson, H., Coluzza, J. (1979) Atmospheric burnup of the Cosmos-954 reactor. Science 205, 583-585.
Kutkov, V., Arefieva, Z., Murav'ev, Y.B., Komaritskaya, O., (1995) Unique form of airborne radioactivity: nuclear fuel'hot particles' released during the Chernobyl accident, Environmental impact of radioactive releases. Proceedings of an international symposium.

Lachner, J., Christl, M., Bisinger, T., Michel, R., Synal, H.-A. (2010) Isotopic signature of plutonium at Bikini atoll. Applied Radiation and Isotopes 68, 979-983.
LaRosa, J., Cooper, E., Ghods-Esphahani, A., Jansta, V., Makarewicz, M., Shawky, S., Vajda, N. (1992) Radiochemical methods used by the IAEA's laboratories at Seibersdorf for the determination of 90Sr, 144Ce and Pu radionuclides in environmental samples collected for the International Chernobyl project. Journal of Environmental Radioactivity 17, 183-209.
Łokas, E., Wachniew, P., Baccolo, G., Gaca, P., Janko, K., Milton, A., Buda, J., Komędera, K., Zawierucha, K. (2022) Unveiling the extreme environmental radioactivity of cryoconite from a Norwegian glacier. Science of The Total Environment 814, 152656.
Łokas, E., Wachniew, P., Jodłowski, P., Gąsiorek, M. (2017) Airborne radionuclides in the proglacial environment as indicators of sources and transfers of soil material. Journal of environmental radioactivity 178, 193-202.
Łokas, E., Zaborska, A., Kolicka, M., Różycki, M., Zawierucha, K. (2016) Accumulation of atmospheric radionuclides and heavy metals in cryoconite holes on an Arctic glacier. Chemosphere 160, 162-172.
Łokas, E., Zaborska, A., Sobota, I., Gaca, P., Milton, J.A., Kocurek, P., Cwanek, A. (2019) Airborne radionuclides and heavy metals in high Arctic terrestrial environment as the indicators of sources and transfers of contamination. The Cryosphere 13, 2075-2086.
Łokas, E., Zawierucha, K., Cwanek, A., Szufa, K., Gaca, P., Mietelski, J.W., Tomankiewicz, E. (2018) The sources of high airborne radioactivity in cryoconite holes from the Caucasus (Georgia). Scientific reports 8, 10802.
Mitchell, P., Vintró, L.L., Dahlgaard, H., Gascó, C., Sánchez-Cabeza, J. (1997) Perturbation in the 240Pu239Pu global fallout ratio in local sediments following the nuclear accidents at Thule (Greenland) and Palomares (Spain). Science of the Total Environment 202, 147-153.
Muramatsu, Y., Hamilton, T., Uchida, S., Tagami, K., Yoshida, S., Robison, W. (2001) Measurement of 240Pu/239Pu isotopic ratios in soils from the Marshall Islands using ICP-MS. Science of the Total Environment 278, 151-159.
Nagar, S., Antony, R., Thamban, M. (2021) Extracellular polymeric substances in Antarctic environments: A review of their ecological roles and impact on glacier biogeochemical cycles. Polar Science 30, 100686.
Olivier, S., Bajo, S., Fifield, L.K., Gäggeler, H.W., Papina, T., Santschi, P.H., Schotterer, U., Schwikowski, M., Wacker, L. (2004) Plutonium from global fallout recorded in an ice core from the Belukha Glacier, Siberian Altai. Environmental science & technology 38, 6507-6512.
Oughton, D.H., Skipperud, L., Fifield, L.K., Cresswell, R.G., Salbu, B., Day, P. (2004) Accelerator mass spectrometry measurement of 240Pu/239Pu isotope ratios in Novaya Zemlya and Kara Sea sediments. Applied Radiation and Isotopes 61, 249-253.
Owens, P.N., Blake, W.H., Millward, G.E. (2019) Extreme levels of fallout radionuclides and other contaminants in glacial sediment (cryoconite) and implications for downstream aquatic ecosystems. Scientific reports 9, 12531.
Pham, M., Sanchez-Cabeza, J., Povinec, P., Andor, K., Arnold, D., Benmansour, M., Bikit, I., Carvalho, F., Dimitrova, K., Edrev, Z. (2008) A new Certified Reference Material for radionuclides in Irish sea sediment (IAEA-385). Applied Radiation and Isotopes 66, 1711-1717.
Pittino, F., Ambrosini, R., Seeger, M., Azzoni, R.S., Diolaiuti, G., Alviz Gazitua, P., Franzetti, A. (2023) Geographical variability of bacterial communities of cryoconite holes of Andean glaciers. Scientific reports 13, 2633.
Povinec, P.P., Aoyama, M., Biddulph, D., Breier, R., Buesseler, K., Chang, C., Golser, R., Hou, X., Ješkovský, M., Jull, A. (2013a) Cesium, iodine and tritium in NW Pacific waters–a comparison of the Fukushima impact with global fallout. Biogeosciences 10, 5481-5496.
Povinec, P.P., Hirose, K., Aoyama, M. (2013b) Fukushima accident: radioactivity impact on the environment. Newnes.

Rääf, C., Holm, E., Rabesiranana, N., Garcia-Tenorio, R., Chamizo, E. (2017) On the presence of plutonium in Madagascar following the SNAP-9A satellite failure. Journal of environmental radioactivity 177, 91-99.
Radiation, I.A.E.A.D.o., Safety, W. (2001) Inventory of accidents and losses at sea involving radioactive material. IAEA.
Roos, P., Holm, E., Persson, R., Aarkrog, A., Nielsen, S. (1994) Deposition of 210Pb, 137Cs, 239+ 240Pu, 238Pu, and 241Am in the Antarctic Peninsula area. Journal of environmental radioactivity 24, 235-251.
Rozwalak, P., Podkowa, P., Buda, J., Niedzielski, P., Kawecki, S., Ambrosini, R., Azzoni, R.S., Baccolo, G., Ceballos, J.L., Cook, J. (2022) Cryoconite–From minerals and organic matter to bioengineered sediments on glacier's surfaces. Science of The Total Environment 807, 150874.
Saito-Kokubu, Y., Yasuda, K., Magara, M., Miyamoto, Y., Sakurai, S., Usuda, S., Yamazaki, H., Yoshikawa, S., Nagaoka, S., Mitamura, M. (2008) Depositional records of plutonium and 137Cs released from Nagasaki atomic bomb in sediment of Nishiyama reservoir at Nagasaki. Journal of environmental radioactivity 99, 211-217.
Sill, C.W. (1987) Precipitation of actinides as fluorides or hydroxides for high-resolution alpha spectrometry. Nuclear and Chemical Waste Management 7, 201-215.
Smith, J., Ellis, K., Naes, K., Dahle, S., Matishov, D. (1995) Sedimentation and mixing rates of radionuclides in Barents Sea sediments off Novaya Zemlya. Deep Sea Research Part II: Topical Studies in Oceanography 42, 1471-1493.
Szufa, K.M., Mietelski, J.W., Anczkiewicz, R., Sala, D., Olech, M.A. (2018) Variations of plutonium isotopic ratios in Antarctic ecosystems. Journal of Radioanalytical and Nuclear Chemistry 318, 1511-1518.
Takeuchi, N., Kohshima, S. (2004) A snow algal community on Tyndall Glacier in the Southern Patagonia Icefield, Chile. Arctic, Antarctic, and Alpine Research 36, 92-99.
Taylor, R.N., Warneke, T., Milton, J.A., Croudace, I.W., Warwick, P.E., Nesbitt, R.W. (2001) Plutonium isotope ratio analysis at femtogram to nanogram levels by multicollector ICP-MS. Journal of Analytical Atomic Spectrometry 16, 279-284.
Tracy, B., Prantl, F., Quinn, J. (1984) Health impact of radioactive debris from the satellite Cosmos 954. Health physics 47, 225-233.
UNSCEAR (1982) Ionizing Radiation, Sources and Biological Effects, United Nations Scientific Committee on the Effects of Atomic Radiation (UNSCEAR) 1982 Report: Report to the General Assembly, with Scientific Annexes. United Nations.
UNSCEAR, (2000) UNSCEAR Report 2000: sources and effects of ionizing radiation.
UNSCEAR, (2010) Sources and effects of ionizing radiation, united nations scientific committee on the effects of atomic radiation (UNSCEAR) 2008 report, volume I: Report to the general assembly, with scientific annexes A and B-sources. United Nations.
Warneke, T., Croudace, I.W., Warwick, P.E., Taylor, R.N. (2002) A new ground-level fallout record of uranium and plutonium isotopes for northern temperate latitudes. Earth and Planetary Science Letters 203, 1047-1057.
Wejnerowski, Ł., Poniecka, E., Buda, J., Klimaszyk, P., Piasecka, A., Dziuba, M.K., Mugnai, G., Takeuchi, N., Zawierucha, K. (2023) Empirical testing of cryoconite granulation: Role of cyanobacteria in the formation of key biogenic structure darkening glaciers in polar regions. Journal of Phycology 59, 939-949.
Wendel, C.C., Oughton, D., Lind, O., Skipperud, L., Fifield, L.K., Isaksson, E., Tims, S., Salbu, B. (2013) Chronology of Pu isotopes and 236U in an Arctic ice core. Science of the total environment 461, 734-741.

Zheng, J., Tagami, K., Uchida, S. (2013) Release of plutonium isotopes into the environment from the Fukushima Daiichi nuclear power plant accident: what is known and what needs to be known. Environmental science & technology 47, 9584-9595.
Zhong, Q., Du, J., Puigcorbé, V., Wang, J., Wang, Q., Deng, B., Zhang, F. (2019) Accumulation of natural and anthropogenic radionuclides in body profiles of Bryidae, a subgroup of mosses. Environmental Science and Pollution Research 26, 27872-27887.